

Spatiotemporal coding in an electrochemical oscillatory network

Yasuyuki Miyakita and Seiichiro Nakabayashi*

Department of Chemistry, Faculty of Science, Saitama University, Saitama City, Saitama 338-8570, Japan

Antonios Karantonis

Department of Materials Science and Engineering, School of Chemical Engineering, National Technical University of Athens, Zografou 15780, Athens, Greece

(Received 8 November 2004; published 20 May 2005)

A network consisting of N relaxation electrochemical oscillators, mutually coupled by all-to-all inhibitory connections, can have $(N-1)!$ coexisting out-of-phase states, each state being a permutation of a periodic spiking sequence. The modification of the out-of-phase states by shots of laser pulse perturbations is shown. In such networks the phase relation of the oscillators is stored as a coded pattern. The ability of the network to function as a rewritable memory of $(N-1)!$ different spatiotemporal patterns is demonstrated experimentally for $N=4$.

DOI: 10.1103/PhysRevE.71.056207

PACS number(s): 82.40.Bj, 05.45.-a

I. INTRODUCTION

Synchronization is a ubiquitous phenomenon in nervous systems. The ability of coupled neurons to synchronize is believed to be one of the possible ways for accomplishing sophisticated actions such as cognition or associative memorization. A number of models have been proposed which treat the concept of associative memory and cognition as a collective property of large interconnected neural networks [1–10]. In many of these models a given set of patterns is embedded in the synaptic interactions between the neurons with their plasticity so as to make these patterns dynamically stable.

There have been several attempts to mimic the memory function in both experiments and simulations. Coupled nonlinear homogeneous chemical reactions were among the first chemical systems capable of performing coding and pattern recognition while in the bistable [11], excitable [12,13], or oscillatory state [14–17]. Coupled multimode lasers [18–20] and coupled Josephson junctions [21] are also nonlinear dynamical systems with this kind of properties, coming from the field of optics and electronics. In this framework also, a given set of spatiotemporal patterns replays as stored information and is induced by external stimuli; however, the network's connections may not change. These networks can function as a prepatterned memory that stores information in the form of spatiotemporal patterns without any synaptic plasticity. Such networks exhibit multiple attractor states, each of which stores the memory of a specific stimulus as a unique persistent pattern. In particular, coupled laser systems have the interesting feature that information is stored as periodic pulse oscillatory sequences. Such states are periodic in time; however, each oscillator is shifted by $1/N$ of the period from its neighbor, where N denotes the number of modes (oscillators). This implies the simultaneous existence of $(N-1)!$ attractors in the phase space where each state can be

selectively excited by applying seed signals; it is thus rewritable [18].

A possible scheme of associative memory and pattern cognition in neural systems is temporal coding which assumes that information is coded in the relative timing of firing pulses [22,23]. In order to study neural properties based on the temporal coding scheme it is imperative to consider each element of the network as capable of oscillating. Based on this fact, our main interest is in oscillatory electrochemical systems where one of the dynamical variables (the potential difference of the electrode/solution interface) is electric in nature similar to the membrane potential of neural cells [24–26]. When firing electrochemical cells communicate through the electrolytic solution the electrode/solution potential difference might become more negative or more positive due to coupling. The first case corresponds to the depolarization (excitatory connection) and the second to the hyperpolarization (inhibitory connection) of a neural membrane.

In a previous work it was demonstrated experimentally, for a network consisting of two electrochemical oscillators, that the action of the connections can be tuned by changing the relative position of the working, counter-, and point reference electrodes under potentiostatic operation [27]. Analysis of the model equations revealed that the coupling function consisted of two terms; one does not have any influence on the coupling dynamics whereas the other can be treated as an instantaneous excitatory or inhibitory connection [27]. As a result, the excitatory and inhibitory connections induce in-phase and out-of-phase synchronization, respectively. In the present work a network consisting of $N=4$ bidirectionally all-to-all inhibitory coupled electrochemical oscillators of relaxation type is considered. Additionally, one or more of the N oscillators are considered to be capable of receiving an external excitatory signal, thus being unidirectionally coupled with the external stimulus in an excitatory manner (Fig. 1). It is demonstrated experimentally that the network has a potentially large capability of storing information in the form of spatially and temporally patterned spiking sequences, which are expressed as specific phase relations be-

*Email address: sei@chem.saitama-u.ac.jp

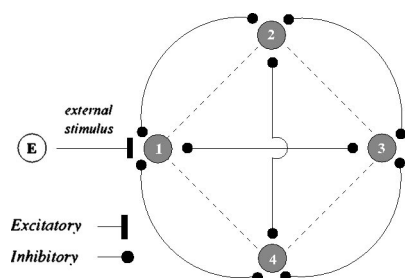


FIG. 1. Schematic representation of a network consisting of $N=4$ oscillators (gray circles) connected through inhibitory connections, together with an external master (white circle) unidirectionally coupled with one of the oscillators through an excitatory connection.

tween the oscillators. In order to explore the network's coding ability an experimental setup is constructed in which N electrochemical oscillators can be driven and monitored as well as perturbed selectively. It is demonstrated that a permutation of a spiking sequence can be selectively induced by applying external excitatory perturbations in the form of laser illuminations.

As an experimental tool the self-sustained current oscillations of relaxation type are utilized during Fe electrodisolution in H_2SO_4 solution. The nonlinear dynamical properties of electrochemical systems have been reviewed extensively in the past [28], and more recently [29] with emphasis on spatial coupling between different sites on electrode surfaces. On the other hand, detailed studies on coupled periodic electrochemical oscillators were performed for the electrodisolution of iron [30–35], cobalt [35–37], and nickel [38], and the reduction of hydrogen peroxide [39,40]. Also a phenomenological resemblance between electrophysiological and electrochemical oscillators has been suggested long ago [41,42], and discussed also in more recent publications [43,44]. Based on this similarity it was recently reported that the dynamical behavior of coupled relaxation electrochemical oscillators has features similar to coupled relaxation neural cells, from the dynamical point of view [24]. It is commonly accepted that the synchronization features of networks of nonlinear oscillatory cells strongly depends on the type of oscillator itself [45–48]. Thus, synchronization of a network consisting of relaxation oscillators is generally archived more rapidly, i.e., within few oscillatory cycles, in contrast to nonrelaxation oscillators. This finding, among others, was found to be true for electrochemical networks. In the present paper, we will also attempt to correlate the coding capability with the relaxation character of the network.

II. EXPERIMENTAL SETUP

The configuration of an assembly consisting of four working electrodes arranged in a square is shown in Fig. 2(a). Each electrode of the assembly was made from pure Fe wires (Nilaco Co., 99.5+%) of 1 mm diameter. The electrodes were embedded in resin in such a way that reaction was taking place only at the end of the Fe wire. For each electrode a cell number was assigned, i.e., 1, 2, 3, and 4. The

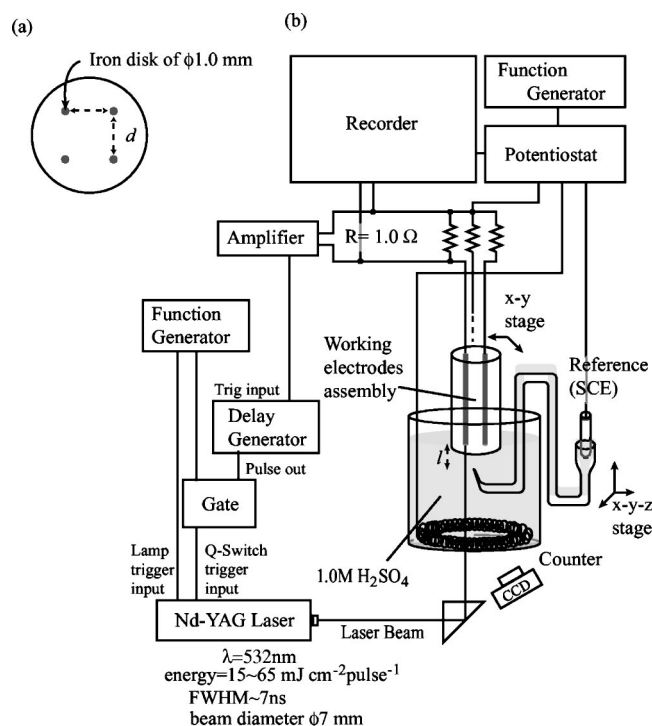


FIG. 2. Schematic illustration of experimental setup: (a) Bottom view of the working electrode assembly consisting of four electrodes arranged in a square with sides d mm long, and (b) illustration and diagram of the electrochemical setup together with the laser system.

distance between electrodes i and j was d_{ij} . Prior to each experiment, the electrodes were polished with a series of wet 200–2000 grit silicon carbide sandpapers, then cleaned with distilled water, and rinsed with ethanol.

The electrode assembly was used as a working electrode in a standard three-electrode arrangement with respect to a Saturated calomel reference electrode (SCE) with a Haber-Luggin capillary. A schematic illustration of the experimental setup of the electrochemical cell together with the measuring and laser system is shown in Fig. 2(b). The tip of the capillary was located at a distance l below the plane of the assembly and as exactly as possible on the central axis of the working assembly by using an x-y-z stage. The counterelectrode was a Cu ring wire parallel to the assembly's surfaces and at a distance of 6 cm. The potential was controlled by a potentiostat (Hokuto Denko, HA-151). The working electrodes were connected to the potentiostat through individual resistors of $1\ \Omega$ in order to measure the response of the electrodes independently. The potential drop on each resistor was measured and stored by using a Memory Hicorder 8441 with four channels analog units 8946 (Hioki E.E. Co.). The experiments were carried out in a 1M H_2SO_4 diluted from concentrated sulfuric acid (Wako Pure Chemical Industries). An additional description of the electrochemical cell arrangement can be found in a previous article [27].

A schematic block diagram of the laser system is also shown in Fig. 2(b). In order to perturb the system, an electrode was illuminated by frequency-doubled light ($\lambda=532\text{ nm}$) from a neodymium-doped yttrium aluminum gar-

net (Nd: YAG) laser (Spectra-Physics, GCR-150). The pulse duration was 7 ns full width at half maximum (FWHM). The energy of each pulse was about $15\text{--}65 \text{ mJ cm}^{-2} \text{ pulse}^{-1}$. The laser was externally driven by a pulse generator (8112A Pulse Generator, HP), generating both a lamp trigger pulse and a Q -switch trigger pulse with frequency 20 Hz. The Q -switch trigger pulse transmitted a gate during a specific time interval that was controlled by using a delay generator (DG535, Stanford Research Systems) triggered by the potential response of the electrode with any desired delay, whereas a flash lamp burned with frequency 20 Hz continuously. Thus, a giant pulse laser was illuminated at desired timing with $\pm 25 \text{ ms}$ resolution. The laser spot was located on the selected electrode as exactly as possible by using an x - y stage. The location of the beam spot was confirmed by using a charge-coupled device camera with long-pulse mode and by monitoring the current response.

III. RESULTS

A. Coupled behavior of the network

A system consisting of only one working electrode exhibits periodic oscillations of relaxation type within an applied potential window extending from $V=245$ to 285 mV . The relaxation limit cycle consists of two main states: a silent state while the electrode is covered by an oxide layer and the current flowing through the cell is small and an active state while the electrode surface is almost oxide-free and a finite current flows. For $V \gtrsim 290 \text{ mV}$ the system lies in a silent steady state whereas for $V < 245 \text{ mV}$ the system lies in an active steady state.

Under the assumption that the phase of the observable coincides with the phase of the oscillator, it is rather trivial to define a phase for a single uncoupled oscillator. Thus, the value $\theta(t)=0$ is attributed to the maximum of the relaxation spike and a phase value is assigned to each point of the observable according to the equation

$$\dot{\theta} = \Omega, \quad (1)$$

where Ω is the frequency of the oscillator and θ is defined in the interval from 0 to 1. Thus, while the observable performs a full cycle, the phase $\theta(t) = [\theta(0) + \Omega t] \pmod{1}$ makes a full rotation around the unit circle with constant speed.

In the case of an assembly of two oscillators, the system response depends on both l and d_{12} , as described in a previous publication [27]; the two electrochemical oscillators can be tuned to be either excitatory or inhibitory by changing the relative position of working and point reference electrodes, l , and this change of the electrodes' action induces stable in-phase or out-of-phase synchronized states, respectively. Analogously, the action of the connections between the electrodes can be tuned even if the number of cells extends to more than two.

In the case of more than one coupled oscillator, it might not be possible to define the phase according to Eq. (1) since the instantaneous frequency $\dot{\theta}$ might differ from Ω . For this purpose, the phase of the i th oscillator is determined by the method of "marker events" [49]; the maxima of the

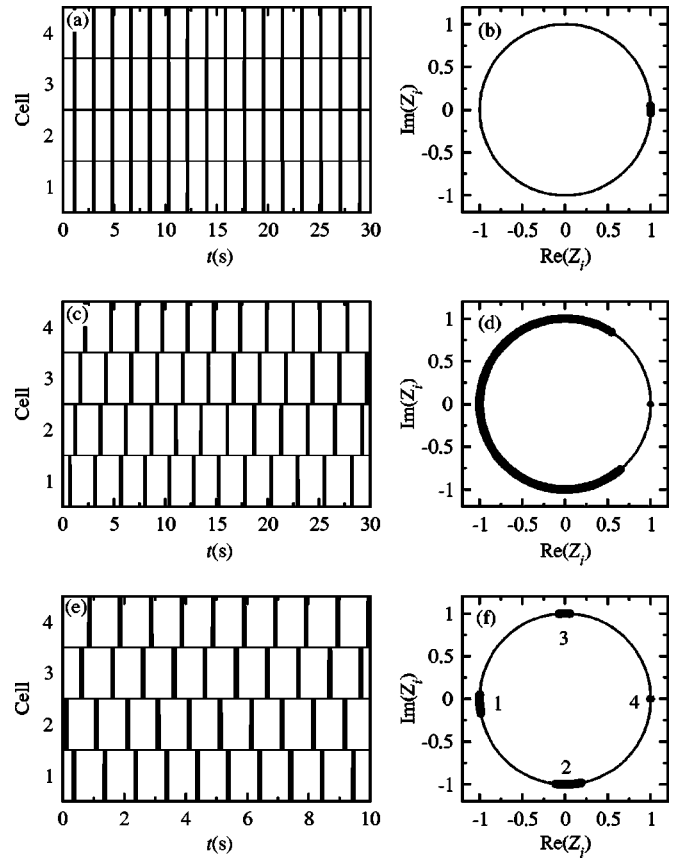


FIG. 3. Synchronization of four oscillators, $N=4$. (a) In-phase synchronization and (b) phase differences in the complex plane for $l=10 \text{ mm}$ and $V=275 \text{ mV}$. (c) Partial synchronization, and (d) phase differences in the complex plane for $l=0 \text{ mm}$ and $V=275 \text{ mV}$. (e) Out-of-phase synchronization and (f) phase differences in the complex plane for $l=0 \text{ mm}$ and $V=262 \text{ mV}$. In all cases $d_{i,i+1}=5 \text{ mm}$ and $d_{i,i+2}=7 \text{ mm}$.

relaxation spikes taking place at times $t_i^{(k)}$, $k=1, 2, \dots$, $i=1, 2, \dots, N$, are assigned to the phase values $\theta_i(t_i^{(k)})=0$ and for any arbitrary instant of time in the interval $(t_i^{(k)}, t_i^{(k+1)})$ the phase is determined as a linear interpolation between these values,

$$\theta_i = \frac{t - t_i^{(k)}}{t_i^{(k+1)} - t_i^{(k)}} \pmod{1}. \quad (2)$$

The other alternative would be to construct a complex process from the scalar time series, by implementing the Hilbert transform [49], a procedure not implemented in the present work.

Let us consider a network consisting of $N=4$ cells arranged in a square with sides $d \text{ mm}$ long in which the oscillators are coupled in nonlocal manner, i.e., the coupling is both next and next-next neighbor. For fixed d and large values of l , where both next and next-next oscillators communicate in an excitatory manner, all four oscillators synchronize in phase for any initial conditions tested experimentally. A representative example of all in-phase synchronization can be seen in Fig. 3(a) for $d=5 \text{ mm}$, $l=10 \text{ mm}$, and V

=275 mV. Here, the binary representation depicts the silent and active states as white and black regions, respectively. Thus, when one electrode is firing the others are excited almost instantly and the phase difference between the oscillators is almost zero.

The phase relation between the cells can be described by the phase differences $\theta_i - \theta_j$. Clearly, all phase differences are not independent; thus we arbitrarily consider χ_i , $i=1, \dots, N$, as

$$\chi_i(t) = [\theta_i(t) - \theta_4(t)] \pmod{1}, \quad (3)$$

where all other phase differences can be generated as combinations of χ_i , $i=1, \dots, N$. Since the unit circle is regarded as $\{e^{2\pi i\theta} | \theta \in \mathbb{R}\}$, where θ is a coordinate modulo 1, both θ_i and χ_i can be represented in the complex plane with coordinates $\text{Re}(Z_i) = \cos(2\pi\theta_i)$ and $\text{Im}(Z_i) = \sin(2\pi\theta_i)$ (similarly for χ_i). As can be seen in Fig. 3(b), the phase differences of the oscillators are almost zero, $\chi_i(t) = 0$, in accordance with the results presented in Fig. 3(a).

For fixed d and small l , where both next and next-next neighbors communicate in an inhibitory manner, the four oscillators never synchronize in phase. On the contrary, the overall response of the network consists of a spiking sequence which is always preserved during the course of measurement. For large applied potential V , the phase difference is not constant, a phenomenon that might have a nonlinear dynamical origin or simply be caused by experimental imperfections. An example of this kind of partial synchronization can be seen in Fig. 3(c) for $d=5$ mm, $l=0$ mm, and $V=275$ mV. All cells oscillate with a phase difference, whereas $\chi_i(t)$ is slowly fluctuating in time. The fluctuation of the phase differences can be seen more profoundly in Fig. 3(d) where $\chi_i(t)$ tends to fill the unit circle. It must be noted that even though $\chi_i(t)$ is varying in time, it is nevertheless bounded (the spiking sequence is preserved); there is thus some kind of coherence in the system.

For smaller values of V , at which the silent state becomes less dominant, a cell is a periodic oscillator with a common period T , but each oscillator is delayed by almost T/N from its neighbor. Thus, $\chi_i(t)$ are fixed during the course of the measurement and the network is synchronized out of phase. A representative example of the spatiotemporal response during out-of-phase synchrony is presented in Fig. 3(e) for $d=5$ mm, $l=0$ mm, and $V=262$ mV. As can be seen, the cells are synchronized and a spiking sequence is preserved in time. The phase differences are presented in Fig. 3(f) where $\chi_1=0.5$, $\chi_2=0.75$, and $\chi_3=0.25$ (obviously, due to the definition of the phase difference, $\chi_4=0$).

Since we are interested in the out-of-phase synchronized state, the transition from partial synchronization to complete synchrony by varying V should be further explored. The dependence of $\chi_i(t)$ on V can be seen more clearly if the applied potential is slowly swept toward decreasing values while the network is partially synchronized. A representative graph showing the time course of $\chi_i(t)$ for $i=1,2,3$ during a cathodic potential sweep (decrease of V from high to low values) is presented in Fig. 4. The range of applied potential at which current oscillations are observed for $N=4$ is not

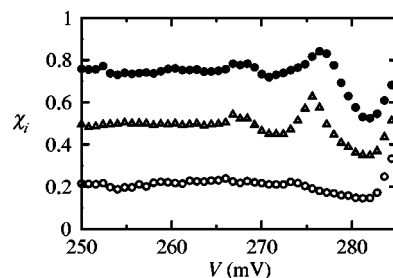


FIG. 4. Plot of phase differences $\chi_i(t)$ versus applied potential V under inhibitory connections for four oscillators during cathodic potential sweep. χ_i , $i=1,2,3$, correspond to the open circle, open triangle, and solid circle, respectively. Scan rate 0.2 mV/s, $d=5$ mm, and $l=0$ mm.

significantly different from the range for a single oscillator. This experimental observation indicates that the dynamical properties of the oscillators are not strongly affected by the presence of the coupling. The oscillations start at ≈ 290 mV; however, near the bifurcation point at which a transition from the silent steady state to a limit cycle occurs, oscillations are not periodic; their apparent period is very large and the firing sequence might change. The firing sequence is preserved as long as cells oscillate periodically within a wide range of V , i.e., from 255 to 280 mV. For large values of V , while keeping other parameters fixed, $\chi_i(t)$ is fluctuating, as in the case of Fig. 3(d).

On the other hand, for small values of V , the phase differences remain fixed, as in Fig. 3(f). The corresponding response of $\chi_i(t)$ for $N=4$ can be seen clearly in Fig. 4. The typical value at which a transition from partial synchronization to out-of-phase synchrony occurs is around 265 mV. Near the bifurcation point from the limit cycle to the active steady state, also the firing sequence might change. However, it must be noticed that over a wide potential range extending from 255 to 265 mV the out-of-phase synchronized state is stable since such a state of constant $\chi_i(t)$ has a duration of several hundreds of oscillatory cycles.

In-phase synchronization corresponds to a state in which all oscillators fire almost simultaneously; thus only one firing sequence exists. However, under inhibitory connections there are $(N-1)!$ out-of-phase states that are distinct. Each of these states corresponds to a circular permutation of a firing sequence, i.e.,

$$\begin{aligned} s_1 &= \{\dots 123412341234\dots\}, \\ s_2 &= \{\dots 142314231423\dots\}, \\ s_3 &= \{\dots 134213421342\dots\}, \\ s_4 &= \{\dots 124312431243\dots\}, \\ s_5 &= \{\dots 132413241324\dots\}, \\ s_6 &= \{\dots 143214321432\dots\}. \end{aligned} \quad (4)$$

In the following, cell 1 is arbitrarily assumed to be the first firing cell in the sequence; hence the repeating patterns cor-

TABLE I. Patterns corresponding to six firing sequences of a four-oscillator network.

Sequence	Pattern	Phase difference $(\chi_1, \chi_2, \chi_3, \chi_4)$
s_1	{1234}	(0.75, 0.5, 0.25, 0)
s_2	{1423}	(0.25, 0.75, 0.5, 0)
s_3	{1342}	(0.5, 0.75, 0.25, 0)
s_4	{1243}	(0.5, 0.25, 0.75, 0)
s_5	{1324}	(0.75, 0.25, 0.5, 0)
s_6	{1432}	(0.25, 0.5, 0.75, 0)

responding to all six firing sequences for a network of four oscillators are those presented in Table I, together with the corresponding phase differences. All other patterns are equivalent to those shown in this table (e.g., sequences {2341} and {1234} both correspond to s_1 since the phase differences are the same). Thus, the result presented in Fig. 3(f) corresponds to the pattern {1342}. Since each pattern corresponds to only one sequence, the two terms will be used without distinction for the rest of the paper. Experimental evidence shows that the firing sequence during stable out-of-phase synchrony depends only on initial conditions or external perturbations. All $(4-1)! = 6$ firing sequences coexist for a network where $N=4$ and were observed by repeating the experiments under the same parameter values but different initial conditions. On the other hand, a small perturbation was able to alter the firing sequence; for example, when the network was synchronized out of phase, the firing sequence was changing by simply stirring the solution for several seconds.

B. Permutation of the spike train by laser perturbations

In the present section, the response of the network under external perturbations is studied in a more systematic way by utilizing a pulse laser beam. Since the iron oxide film has n -type semiconducting properties a photo-created hole in the valence band destroys the lattice of the film [50] and thus eliminates the silent state. The elimination of the silent state corresponds to a decrease of the double layer potential and thus to excitation. The action of the laser beam can be viewed also as unidirectional excitatory coupling between a slave (the electrochemical oscillator) and a master (the laser source). The use of a laser beam allows us to introduce external perturbations into the network in a systematic way. Also the timing of such pulse laser beams can be controlled with good accuracy; thus a desired cell can be perturbed at specific time instants. Additionally, the laser impact is not expected to have any effect on other parameters of the system.

The response of single iron electrochemical oscillators under laser perturbation has been investigated to some extent in the past [51,52]. As a first step, let us consider the response of a single cell under laser perturbations in the present experimental conditions. As before, the instant of autonomous activation is considered as the reference event, $t=0$. A laser pulse is perturbing the cell at the time instant t_p ;

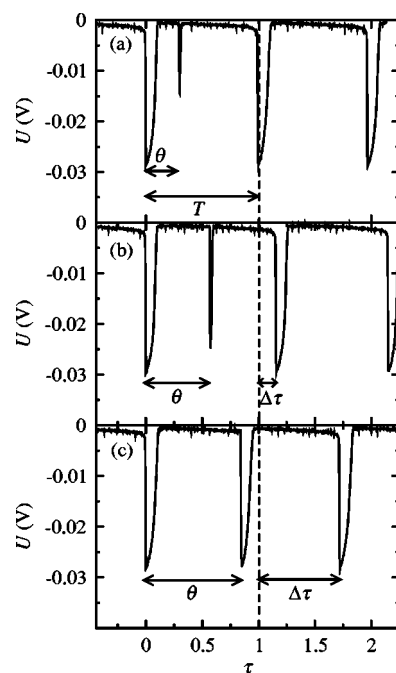


FIG. 5. Effect of a single laser perturbation on an isolated oscillator. Time is normalized with respect to the autonomous period T . (a) For a perturbation within the refractory region, $\theta=0.3$, a spike is induced but there is no increase of the period, $\Delta\tau=0$. (b) For a perturbation within the excitable region, $\theta=0.57$, a spike is induced and the period is increased, $\Delta\tau=0.16$ and (c) $\theta=0.85$, $\Delta\tau=0.72$.

the response of the cell is mainly determined by this time instant. Above a critical value of pulse energy, no significant difference is observed in consistency with earlier work [52]. The typical threshold energy is $15\text{--}35 \text{ mJ cm}^{-2} \text{ pulse}^{-1}$. Experimental evidence suggests that within an oscillatory cycle, two regions exist: a refractory and an excitable region. Within the refractory region small sharp current peaks are induced and the period of the cycle remains more or less unaffected. If the laser pulse is applied while in the excitable region, a large peak of almost the same amplitude to the autonomous peak is induced and the period of the autonomous cycle is increased by Δt , within the cycle in which the perturbation is applied. Thus, the main effect of the perturbation is to delay the oscillator and this delay is determined by the phase of the perturbed oscillation at the instant t_p . An example of the effect of perturbation for a single cell is shown in Fig. 5. As can be seen in this figure, when the perturbation is applied while the phase of the oscillator is small, a sharp spike is induced but the period of the perturbed cycle remains unaffected and a phase shift is not observed [Fig. 5(a) for $\theta=0.3$]. On the other hand, when the phase is larger [e.g., $\theta=0.57$ and 0.85 in Figs. 5(b) and 5(c)] the perturbation induces a large spike, the period is increased by $\Delta\tau=0.16$ and 0.72 , respectively, and the oscillator is delayed. The new phase after a single perturbation is given by

$$\phi(\theta) = \theta - \Delta\tau(\theta) \pmod{1}, \quad (5)$$

where θ is given by either Eq. (1) or (2). The dependence of $\Delta\tau$ on θ can be seen in Fig. 6. When the laser pulse is

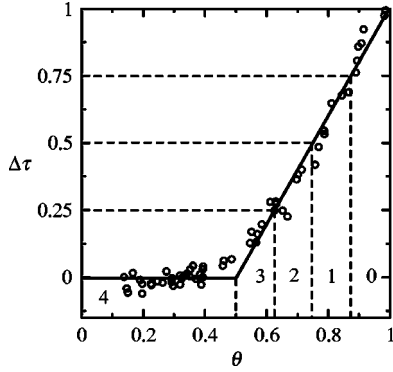


FIG. 6. Dependence of $\Delta\tau$ on θ . Zones 1, 2, and 3 correspond to the advance of the perturbed cell over one, two, and three cells, respectively. Zone 0 corresponds to no advance and zone 4 to the refractory region.

illuminating under a critical phase value (in this case around $\theta=0.5$), $\Delta\tau$ is approximately equal to 0, whereas above the critical value of phase, $\Delta\tau$ monotonically increases on increasing θ . In this graph, the region $\theta \geq 0.5$ is fitted by a linear function for convenience, even though the relation might be nonlinear.

The response of a network consisting of more than one cell under single perturbation can be predicted to some extent by the above relation. Hence, the following sequence of events is expected to occur. (a) The cells oscillate out of phase and the advance of cell i over cell j corresponds to a phase shift equal to $\chi_i - \chi_j = 0.25$. (b) At a specific time instant cell i is perturbed. As a result its period within the perturbed cycle is extended by an amount $\Delta\tau(\theta_i)$. (c) Due to the extension of the period, cell i is delayed according to Eq. (5). (d) Cell i fires an autonomous delayed spike. A new phase relation is determined between the cells, depending on $\phi_i(\theta_i)$. (e) Due to inhibition, all cells arrange their phase in order to preserve the 0.25 phase shift. This arrangement occurs rapidly due to the relaxation character of the oscillations.

Let us consider a network synchronized out of phase where the firing sequence is $\{iklm\}$ with phase differences $\chi_i=0.75$, $\chi_k=0.5$, $\chi_l=0.25$, and $\chi_m=0$. By using Eqs. (3) and (5), the phase difference after a single perturbation on cell i will be

$$\tilde{\chi}_i = \chi_i - \Delta\tau \pmod{1}. \quad (6)$$

Equation (6) indicates the following.

(a) If $0.75 < \Delta\tau < 1$ then $\chi_i < \tilde{\chi}_i < \chi_m$. Cell i fires a delayed autonomous spike after m and before k . The phase relation is preserved.

(b) If $0.5 < \Delta\tau < 0.75$ then $\chi_m < \tilde{\chi}_i < \chi_l$. Cell i fires a delayed autonomous spike after l and before m . Hence, cell i is advancing over m .

(c) If $0.25 < \Delta\tau < 0.5$ then $\chi_l < \tilde{\chi}_i < \chi_k$. Cell i fires a delayed autonomous spike after k and before l . Hence, cell i is advancing over both m and l .

Hence, according to the above, the graph of Fig. 6 can be divided into several distinct zones. Zone 0 corresponds to phase values θ for which $\Delta\tau > \chi_i$ and the firing sequence is

preserved under the influence of perturbations, even though the perturbation induces a phase shift. Zone 1 corresponds to those values of θ for which $\chi_k < \Delta\tau < \chi_i$ and perturbation on cell i causes this cell to advance over the next cell. Zone 2 corresponds to θ values for which $\chi_l < \Delta\tau < \chi_k$ and perturbation on cell i causes this cell to advance over the two next cells. Zone 3 presents nothing new, since advancing over all the following cells leads to the same firing sequence due to symmetry. Finally, zone 4 corresponds to those values of θ for which a phase shift is not observed (refractory region).

If we assume that for zone 1 a mapping $\sigma_1(s_i)$ exists due to the action of a perturbation on a single cell i , the following transitions are expected:

$$\begin{array}{c} \sigma_1 \quad \sigma_1 \quad \sigma_1 \\ s_1 \rightarrow s_2 \rightarrow s_3 \rightarrow s_1, \end{array}$$

$$\begin{array}{c} \sigma_1 \quad \sigma_1 \quad \sigma_1 \\ s_4 \rightarrow s_5 \rightarrow s_6 \rightarrow s_4, \quad \text{zone 1.} \end{array} \quad (7)$$

In a similar manner if $\sigma_2(s_i)$ corresponds to zone 2, then the transitions are

$$\begin{array}{c} \sigma_2 \quad \sigma_2 \quad \sigma_2 \\ s_1 \rightarrow s_3 \rightarrow s_2 \rightarrow s_1, \end{array}$$

$$\begin{array}{c} \sigma_2 \quad \sigma_2 \quad \sigma_2 \\ s_4 \rightarrow s_6 \rightarrow s_5 \rightarrow s_4, \quad \text{zone 2.} \end{array} \quad (8)$$

By comparing Eqs. (7) and (8) it can be observed that $\sigma_2(s_i) = \sigma_1(\sigma_1(s_i)) \equiv \sigma_1^2(s_i)$. It must be noticed also that the altering of firing sequences is expected to occur rapidly (within a few cycles) due to the relaxation character of the oscillators.

In Fig. 7(a) an example is presented for a perturbation applied within zone 0. As can be seen, initially the sequence is s_4 corresponding to the pattern $\{1243\}$. At $\theta=0.89$ a perturbation is applied and as a result a large spike is induced (dashed region). Nevertheless, the firing sequence is not altered since for this value of θ the time delay corresponds to $\Delta\tau > 0.75$ (see Fig. 6). This is in contrast to the result presented in Fig. 7(b) where the perturbation is applied at $\theta=0.8$. In this case, the initial pattern is $\{1324\}$, that is, the sequence is s_5 . By inspecting Fig. 6 it can be seen that this value of θ belongs to zone 1 and according to Eq. (7), $\sigma_1(s_5) = s_6$. This is indeed the case, since the resulting pattern is $\{1432\}$. Finally, an example of a perturbation causing the advance over two cells is presented in Fig. 7(c). In this case $\theta=0.71$ and thus belongs to zone 2. Initially the sequence is s_5 (pattern $\{1324\}$). According to Eq. (8), $\sigma_2(s_5) = s_4$. Indeed, once the perturbation is applied the resulting sequence is $\{1243\}$.

Let us explore further the response of the network for a perturbation belonging to zone 1. For small l and small N within the oscillatory region the network is synchronized out of phase and the time delay between the cells is T/N . Under these conditions a network consisting of four oscillators has $(4-1)!$ stable states, manifested as a permutation of a spiking sequence. The spiking sequence depends only on the initial conditions and external perturbations. A laser pulse illuminating only a specific cell at a specific time instant can modify the permutation of the spiking sequence if

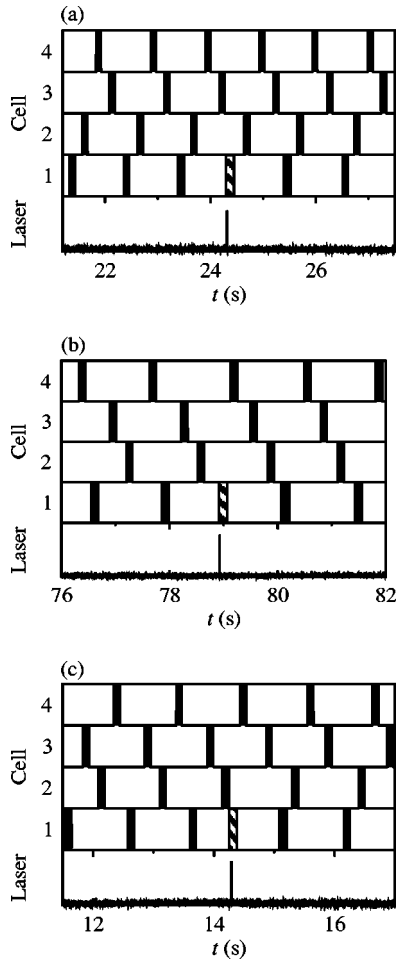


FIG. 7. (a) Zone 0: Perturbation on the sequence s_4 (pattern $\{1243\}$) at $\theta=0.89$; the sequence is preserved. (b) Zone 1: Perturbation on s_5 at $\theta=0.8$ and resulting sequence s_6 ; the pattern $\{1324\}$ transforms to $\{1432\}$. (c) Zone 2: Perturbation on the sequence s_5 at $\theta=0.71$ and resulting sequence s_4 ; the pattern $\{1324\}$ transforms to $\{1243\}$. The dashed region corresponds to an induced spike due to the laser pulse, shown at the bottom of each graph.

it is applied within the excitable region of the oscillatory cycle and within zones 1 and 2. In the specific case of zone 1, the spiking sequence can be altered by a series of perturbations within different oscillatory cycles as shown in Fig. 8. A graph showing the initial sequence s_6 , corresponding to the pattern $\{1432\}$, is presented in Fig. 8(a). When $t=18.9$ s a perturbation is applied to cell 1 while its phase is $\theta=0.78$. As a result the transition $\sigma_1(s_6)=s_4$ is observed and the pattern transforms to $\{1243\}$ [Fig. 8(b)]. As the network continues to oscillate with this firing sequence, a perturbation is applied at $t=48.9$ s while the phase of cell 1 is $\theta=0.79$. Due to the perturbation the transition $\sigma_1(s_4)=s_5$ takes place and the resulting sequence, presented in Fig. 8(c), is $\{1324\}$. From this time on, the system fires with this time sequence until another perturbation is applied at $t=78.9$ s while the phase of cell 1 is $\theta=0.77$. The perturbation induces a transition $\sigma_1(s_5)=s_6$ and the pattern $\{1432\}$ is introduced as shown in Fig. 8(d). This sequence is exactly the same as the initial one, Fig. 8(a). Finally, when a perturbation is applied to cell 1 at $t=108.9$ s, when the phase is $\theta=0.79$, the transition $\sigma_1(s_6)$

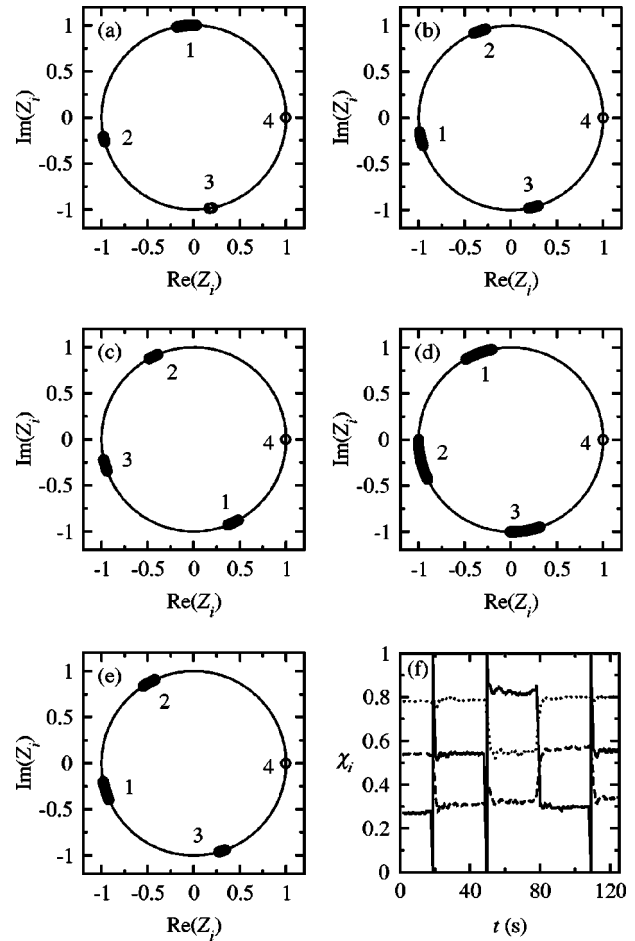


FIG. 8. Sequential transitions to different firing sequences under the influence of repeated single laser perturbations on cell 1 at $t = 18.9, 48.9, 78.9,$ and 108.9 s. (a) Initial sequence s_6 corresponding to a pattern $\{1432\}$, (b) transition $\sigma_1(s_6)=s_4$, (c) transition $\sigma_1(s_4)=s_5$, (d) transition $\sigma_1(s_5)=s_6$, (e) transition $\sigma_1(s_6)=s_4$, and (f) corresponding time evolution of χ_i where $i=1,2,3$ correspond to the full, dashed, and dotted curves, respectively.

$=s_4$ is observed and the firing pattern becomes $\{1243\}$ [Fig. 8(e)], which is the same as the one presented in Fig. 8(b). The overall variation of the phase differences χ_i in the course of time under the influence of single perturbations of cell 1 at $t=18.9, 48.9, 78.9,$ and 108.9 s can be seen also in Fig. 8(f).

Apparently, in Fig. 8 only three different firing sequences are present in accordance with Eq. (7). Apparently, transitions between all $(N-1)! = 6$ states require multiple perturbations on at least two different cells. However, it can be stated that a permutation of the firing sequence can be induced selectively by applying laser perturbations on the appropriate cells. In this network, a given set of synchronization modes coexist (different firing sequences) which can be considered as coded sequences of prestored symbols. The sequences can be induced by external inputs and thus the network functions as a memory of those prestored patterns.

IV. DISCUSSION

Pioneering work on coupled bistable or oscillatory chemical reactions [11,14–17] revealed that indeed such systems

have the ability to mimic coding and memory functions. In the present paper, each element of the electrochemical network is an oscillator instead of a bistable element in order to satisfy the conditions of the temporal coding hypothesis according to which information is coded in the relative timing of firing pulses. Moreover, in a network of electrochemical oscillators one of the dynamical variables is the electric potential of the electrode/solution interface, in analogy to the membrane potential of neural cells. This is in contrast to previous publications [14–17] where even though the chemical reactors were electrically coupled, the potential was externally imposed and none of the dynamical variables of the system was electric in nature.

The ability of a network of N relaxation electrochemical oscillators to prestore $(N-1)!$ firing sequences is based on the assembly's ability to synchronize out of phase. This is different from the coupled multimode laser system based on antiphase synchrony [18].

In order to observe stable out-of-phase synchrony, the cells should be all-to-all coupled in an inhibitory manner. For a network consisting of $N=4$ oscillators this can be achieved if the reference electrode is located close enough to the assembly, for reasons discussed in a previous publication [27]. This interesting property has also been pointed out when spatiotemporal pattern formation was studied in continuous electrochemical systems [35,53–56]. In the case of a continuous electrochemical system, the position of a point reference electrode determines whether nonlocal coupling is positive (excitatory) or negative (inhibitory). In the former case, coupling tends to homogenize the surface whereas in the latter case it introduces an inhomogeneity.

In the present work, inhibitory coupling is utilized for a discrete network of $N=4$ oscillators in order to have a multistable system where each of the $(N-1)!=6$ stable states represents a unique firing sequence. Each state of stable out-of-phase synchrony persists within a wide range of applied potential. A question arises of whether a network consisting of $N>4$ oscillatory cells can also have $(N-1)!$ coexisting stable firing sequences. The same question has also been discussed in the context of coupled multimode laser systems [18,19]. It was pointed out that $(N-1)!$ antiphase states tend to coexist with other attractors such as chaotic orbits and clustered states when the number of modes N is increased, due to the shrinking of the attraction basin of antiphase states and the expansion of the attraction basin of other orbits. In our system, the range of applied potential (the control parameter) at which relaxation oscillations are observed for the coupled system is not significantly different from that of the uncoupled system. This is an indication that the dynamical features of the oscillators are not strongly modified due to coupling; thus other attractors such as fixed points and chaotic orbits might not be newly created in the phase space. This is in good agreement with the experimental fact that for

$N=4$ the range of applied potential at which out-of-phase synchrony is observed is not very different from the range at which periodic relaxation oscillations are observed. Additionally, out-of-phase synchrony within the oscillatory regime is the only observable stable state for the present system. The ability to observe sustain oscillations under coupling is also known to be an additional synchronization advantage for relaxation oscillators [45]. In spite of the technical difficulties, it is intuitively expected that, up to some value of N , $(N-1)!$ firing sequences will coexist as long as all N cells are coupled in an inhibitory manner. However, to answer the question precisely, further investigation, both experimental and theoretical, is needed.

In order to retrieve each of the firing sequences, one or more cells have to be perturbed while in the appropriate phase. Here, cells were perturbed in an excitatory manner by using a laser beam. This perturbation increases the period of the perturbed cell within the cycle where it is applied. As a result, the perturbed cell is delayed. Since this delay is determined by the phase of the cell at the instant of perturbation, the retrieved firing sequence can be predicted or produced at will. It is expected that a similar effect could be observed with an inhibitory instead of an excitatory perturbation, if its effect were to alter the period of the oscillator only within the cycle where it was applied and if the induced period change were determined by the phase of the perturbed cell.

The ability of the network to synchronize rather rapidly out of phase is attributed mainly to the relaxation character of the oscillators. Due to these relatively fast transitions the system responds rapidly to external input and adjusts the phase differences to new firing sequences within several oscillatory cycles.

As a conclusion, the network of electrochemical oscillators presented in this paper has the following properties: (a) the oscillations are of relaxation type, (b) the coupling is all-to-all inhibitory, and (c) the external perturbation alters the period of one oscillatory cycle. Feature (a) ensures relatively fast transition to stable synchronized states and elimination of small differences between the oscillators. Feature (b) induces stable out-of-phase synchronized states, expressed as distinct firing sequences (spatiotemporal coded patterns). Finally, feature (c) allows the retrieval of coded patterns and controllable transitions between different firing sequences.

ACKNOWLEDGMENTS

The work was sponsored by the Greek Secretariat of Research and Technology and the Op. P. "Com." The constant support and encouragement of Professor Y. Chrysosoulakis to A.K. is specially acknowledged. One of the authors, Y.M., is supported by the Japan Society for the Promotion of Science for Young Scientists.

- [1] H. Haken, *Principles of Brain Functioning: A Synergetic Approach to Brain Activity, Behavior and Cognition*, Springer Series in Synergetics Vol. 67 (Springer-Verlag, Berlin, 1996).
- [2] J. J. Hopfield, Proc. Natl. Acad. Sci. U.S.A. **79**, 2554 (1982).
- [3] J. J. Hopfield, Proc. Natl. Acad. Sci. U.S.A. **81**, 3088 (1984).
- [4] D. J. Amit, H. Gutfreund, and H. Sompolinsky, Phys. Rev. Lett. **55**, 1530 (1985).
- [5] D. J. Amit, H. Gutfreund, and H. Sompolinsky, Phys. Rev. A **35**, 2293 (1987).
- [6] K. Nakamura and M. Nakagawa, J. Phys. Soc. Jpn. **62**, 2942 (1993).
- [7] E. M. Izhikevich, IEEE Trans. Neural Netw. **10**, 508 (1999).
- [8] N. Schinor and F. Schneider, Phys. Chem. Chem. Phys. **3**, 4060 (2001).
- [9] H. Hasegawa, J. Phys. Soc. Jpn. **70**, 2210 (2001).
- [10] M. Yoshida and H. Hayashi, Phys. Rev. E **69**, 011910 (2004).
- [11] J.-P. Laplante, M. Pamberton, A. Hjelmelt, and J. Ross, J. Phys. Chem. **99**, 10063 (1995).
- [12] I. N. Motoike, K. Yoshikawa, Y. Iguchi, and S. Nakata, Phys. Rev. E **63**, 036220 (2001).
- [13] I. Motoike and K. Yoshikawa, Phys. Rev. E **59**, 5354 (1999).
- [14] G. Dechert, K.-P. Zeyer, D. Labender, and F. W. Schneider, J. Phys. Chem. **100**, 19043 (1996).
- [15] W. Hohmann, M. Kraus, and F. W. Schneider, J. Phys. Chem. A **101**, 7364 (1998).
- [16] W. Hohmann, M. Kraus, and F. W. Schneider, J. Phys. Chem. A **102**, 3103 (1998).
- [17] W. Hohmann, M. Kraus, and F. W. Schneider, J. Phys. Chem. A **103**, 7606 (1999).
- [18] K. Otsuka, Phys. Rev. Lett. **67**, 1090 (1991).
- [19] K. Otsuka and J.-L. Chern, Phys. Rev. A **45**, 8288 (1992).
- [20] K. Wiesenfeld, C. Bracikowski, G. James, and R. Roy, Phys. Rev. Lett. **65**, 1749 (1990).
- [21] I. B. Schwartz and K. Y. Tsang, Phys. Rev. Lett. **73**, 2797 (1994).
- [22] C. M. Gray, P. König, A. K. Engel, and W. Singer, Nature (London) **338**, 334 (1989).
- [23] E. Vaadia, I. Haalman, M. Abeles, H. Bergman, Y. Prut, H. Slovin, and A. Aertsen, Nature (London) **373**, 515 (1995).
- [24] A. Karantonis, Y. Miyakita, and S. Nakabayashi, Phys. Rev. E **65**, 046213 (2002).
- [25] Y. Miyakita, A. Karantonis, and S. Nakabayashi, Chem. Phys. Lett. **362**, 461 (2002).
- [26] A. Karantonis, M. Pagitsas, Y. Miyakita, and S. Nakabayashi, J. Phys. Chem. B **108**, 5836 (2004).
- [27] A. Karantonis, M. Pagitsas, Y. Miyakita, and S. Nakabayashi, J. Phys. Chem. B **107**, 14622 (2003).
- [28] J. L. Hudson and T. T. Tsotsis, Chem. Eng. Sci. **49**, 1493 (1994).
- [29] K. Krischer, J. Electroanal. Chem. **501**, 1 (2001).
- [30] Y. Wang and J. L. Hudson, J. Phys. Chem. **96**, 8667 (1992).
- [31] Z. Fei, R. G. Kelly, and J. L. Hudson, J. Phys. Chem. **100**, 18986 (1996).
- [32] S. Nakabayashi, K. Zama, and K. Uosaki, J. Electrochem. Soc. **143**, 2258 (1996).
- [33] Z. Fei and J. L. Hudson, J. Phys. Chem. B **101**, 10356 (1997).
- [34] Z. Fei, B. J. Green, and J. L. Hudson, J. Phys. Chem. B **103**, 2178 (1999).
- [35] N. I. Jaeger, R. D. Otterstedt, A. Bírzu, B. J. Green, and J. L. Hudson, Chaos **12**, 231 (2002).
- [36] J. C. Bell, N. I. Jaeger, and J. L. Hudson, J. Phys. Chem. **96**, 8671 (1992).
- [37] R. D. Otterstedt, N. I. Jaeger, P. J. Plath, and J. L. Hudson, Chem. Eng. Sci. **54**, 1221 (1999).
- [38] I. Z. Kiss, W. Wang, and J. L. Hudson, J. Phys. Chem. B **103**, 11433 (1999).
- [39] Y. Mukouyama, H. Hommura, T. Matsuda, S. Yae, and T. Nakato, Chem. Lett. **1996**, 463 (1996).
- [40] T. Matsuda, Y. Mukouyama, H. Hommura, S. Yae, and Y. Nakato, J. Electrochem. Soc. **144**, 2996 (1997).
- [41] W. Ostwald, Z. Phys. Chem., Stoechiom. Verwandtschaftsl. **35**, 333 (1900).
- [42] U. F. Franck, Prog. Biophys. Biophys. Chem. **6**, 171 (1956).
- [43] H. Okamoto, N. Tanaka, and M. Naito, Chem. Phys. Lett. **237**, 432 (1995).
- [44] C. Amatore, A. R. Brown, L. Thouin, and J.-S. Warkocz, C.R. Acad. Sci., Ser. IIC: Chim **1**, 509 (1998).
- [45] D. Somers and N. Kopell, Biol. Cybern. **68**, 393 (1993).
- [46] E. M. Izhikevich, SIAM J. Appl. Math. **60**, 1789 (2000).
- [47] D. Wang and D. Terman, IEEE Trans. Neural Netw. **6**, 283 (1995).
- [48] D. Terman and D. Wang, Physica D **81**, 148 (1995).
- [49] A. Pikovsky, M. Rosenblum, and J. Kurths, *Synchronization: A Universal Concept in Nonlinear Sciences*, Cambridge Nonlinear Science Series Vol. 12 (Cambridge University Press, Cambridge, U.K., 2001).
- [50] K. L. Hardee and A. J. Bard, J. Electrochem. Soc. **123**, 1024 (1976).
- [51] A. Karantonis, Y. Shiomi, and S. Nakabayashi, Int. J. Bifurcation Chaos Appl. Sci. Eng. **11**, 1275 (2001).
- [52] A. Karantonis, Y. Shiomi, and S. Nakabayashi, Chem. Phys. Lett. **335**, 221 (2001).
- [53] J. Christoph, R. D. Otterstedt, M. Eiswirth, N. I. Jaeger, and J. L. Hudson, J. Chem. Phys. **110**, 8614 (1999).
- [54] A. Bírzu, B. J. Green, R. D. Otterstedt, N. I. Jaeger, and J. L. Hudson, Phys. Chem. Chem. Phys. **2**, 2715 (2000).
- [55] A. Bírzu, B. J. Green, N. I. Jaeger, and J. L. Hudson, J. Electroanal. Chem. **504**, 126 (2001).
- [56] A. Bírzu, B. J. Green, R. D. Otterstedt, J. L. Hudson, and N. I. Jaeger, Z. Phys. Chem. (Munich) **216**, 459 (2002).